Materials Today Bio 25 (2024) 100999

Contents lists available at ScienceDirect

Materials Today Bio

journal homepage: www.journals.elsevier.com/materials-today-bio

"*In-situ*" formation of elastin-like recombinamer hydrogels with tunable viscoelasticity through efficient one-pot process

M. Hamed Misbah [a], Luis Quintanilla-Sierra [b], Matilde Alonso [b], José Carlos Rodríguez-Cabello [b], Mercedes Santos [b,*]

[a] *Nanoscience Department, Institute of Nanoscience & Nanotechnology, Kafrelsheikh University, Kafrelsheikh, 33511, Egypt*
[b] *G.I.R. Bioforge, University of Valladolid, CIBER-BBN, Paseo de Belén 19, 47011, Valladolid, Spain*

ARTICLE INFO

Keywords:
ELRs
Hydrogel
Amidation reaction
Viscoelastic

ABSTRACT

Despite the remarkable progress in the generation of recombinant elastin-like (ELR) hydrogels, further improvements are still required to enhance and control their viscoelasticity, as well as limit the use of expensive chemical reagents, time-consuming processes and several purification steps. To alleviate this issue, the reactivity of carboxylic groups from glutamic (E) acid distributed along the hydrophilic block of an amphiphilic ELR (coded as E50I60) with amine groups has been studied through a one-pot amidation reaction in aqueous solutions, for the first time. By means of this approach, immediate conjugation of E50I60 with molecules containing amine groups has been performed with a high yield, as demonstrated by the ^{1}H NMR and MALDI-TOF spectroscopies. This has resulted in the preparation of viscoelastic irreversible hydrogels through the "*in-situ*" cross-linking of E50I60 with another ELR (coded as VKV24) containing amine groups from lysines (K). The rheology analysis demonstrated that the gelation process takes place following a dual mechanism dependent on the ELR concentration: physical cross-linking of I60 block through the hydrophobic interactions, and covalent cross-linking of E50I60 with VKV24 through the amidation reaction. While the chemical network formed between the hydrophilic E50 block and VKV24 ELR preserves the elasticity of ELR hydrogels, the self-assembly of the I60 block through the hydrophobic interactions provides a tunable physical network. The presented investigation serves as a basis for generating ELR hydrogels with tunable viscoelastic properties promising for tissue regeneration, through an "*in-situ*", rapid, scalable, economically and feasible one-pot method.

1. Introduction

Viscoelastic hydrogels with tunable properties have attracted attention for various biomedical and biotechnological applications such as drug delivery, wound sealing, hemostasis and tissue regeneration (bone, enamel and inter-vertebrate disc regeneration) [1–6]. These hydrogels are developed based on the synergistic combination of physical and covalent networks to combine the properties of elastic solids and viscous liquids [4,7–9]. Among those polymeric materials that are characterized by extraordinary supramolecular interactions for physical cross-linking, as well as by the presence of functional groups along its monomer chain necessary for chemical cross-linking, are the modular nature of genetically encoded simulated proteins [1,9,10]. For instance, the self-assembly properties of elastin-like recombinamers (ELRs) in aqueous solutions can be tailored to generate complex one-, two- and three-dimensional structures by means of bottom-up approach, as the desired amino acids sequences and/or bioactive domains are well-constructed with the high precision of molecular weight [10–14].

The key parameter of the ELR self-assembly properties is the reversible phase transition of their chains from disordered to ordered states at a critical temperature (T_t), in aqueous solutions [10,12–16]. While the ELRs chains lack typical secondary structures (α-helix, β-sheet, etc.) below the T_t, they can be folded into an ordered/organized structure above the T_t. The value of T_t depends on the polarity of the guest amino acid X in their penta-peptide sequence (VPGXG), (V = L-valine, P = L-proline, and G = glycine, with X being any amino acid except L-proline). For example, the substitution of X-amino acid by L-isoleucine (I) can result in the generation of poly(VPGIG) with a hydrophobic nature [17,18]. On the contrary, L-glutamic (E) and L-lysine (K) give rise to poly(VPGEG) and poly(VPGKG) with a hydrophilic nature [18–20]. Indeed, the combination of MESLLP$((VPGVG)_2(VPGEG)(VPGVG)_2))_{10}$ (E50) with the $(VGIPG)_{60}$V (I60) can result in the formation of

* Corresponding author.
E-mail address: msantos@bioforge.uva.es (M. Santos).

https://doi.org/10.1016/j.mtbio.2024.100999
Received 3 October 2023; Received in revised form 8 February 2024; Accepted 9 February 2024
Available online 10 February 2024

amphiphilic E50I60 ELR chains [13,21]. In aqueous solution, these amphiphilic chains can assemble with each other into a micellar nanostructure, such that the hydrophobic I60 block forms the core, while the hydrophilic E50 block forms the corona. Furthermore, the self-assembled E50I60 ELR nanostructure can be organized into three-dimensional networks through hydrophobic interaction, but is still reversible when placed below the intrinsic T_t of ELR chain. To stabilize these structures, various sequences inspired by silk or leucine zipper proteins have been introduced to the ELRs chain to generate irreversible physically cross-linked hydrogels [22,23]. However, the uncontrollable gelation speed still limits the ELRs applications. In this regard, chemically cross-linked ELR chains through the amine groups found on the guest X amino acid have gained attention to generate hierarchical structures and/or hydrogel networks [24,25]. For instance, cross-linkers such as glutaraldehyde (GTA) [26,27], bis(sulfosuccinimidyl) suberate (BS3) [27], tris-succinimidyl aminotriacetate (TSAT) [27–29], β-[tris(hydroxymethyl)phosphino]propionic acid (THPP) [29,30], pyrroloquinoline quinone (PQQ) [31], hydroxymethylphosphines (HMPs) [32] have been used to generate hydrogel networks. However, some of these cross-linkers are limited by the achievement of inhomogeneous cross-linking and by their potential toxicity [25,32,33].

Although the self-assembly characteristics of ELRs chains in aqueous solution differ significantly from those observed in organic solvents, the chemical modification of ELRs chains are frequently performed in organic solvents and only using the amine groups (not the carboxylic groups) found along the ELR chains. For example, a chemical cross-linking strategy has been developed in advance that includes a two-step process [20,34,35]. The first step is the modification of the amine groups along the ELRs chains with the desired reactive groups in organic solvent, and the second step is the cross-linking of the chemically modified ELRs in aqueous solutions. For instance, the amine groups found in the K lysine residues of (VPGKG) were first modified to obtain two separate ELRs functionalized with two different reactive groups—one carrying azide groups and the other carrying activated alkyne groups (e.g., cyclooctyne). The mixing of these functionalized ELRs at physiological conditions results in a rapid hydrogel formation by the way of catalyst-free click chemistry (azide−alkyne [3 + 2] cycloaddition) [20]. Also, the K residues on the ELR chains can be modified with methacrylate groups, which are photo-cross-linked in the presence of a photo-initiator [36]. Although these preparation methods are characterized by their selectivity and the controlled modification reaction rate in addition to the biocompatibility of the obtained hydrogel matrices, the chemical modification of the amine groups on K residues is performed in organic solvent and requires expensive chemical reagents, time-consuming processes and several purification steps. Furthermore, the chemical modification of amine groups has resulted in decreasing the value of T_t and, therefore, increasing the hydrophobicity of the ELR chains [20,34–36]. This results in reducing the water solubility of the chemically modified ELRs chains, which limits their applicability when used to prepare hydrogels. This in consequence affects the self-assembly and viscoelastic properties in comparison to their unmodified counterparts. In order to ensure the preservations of the characteristic self-assembly, organization, and viscoelastic properties prior to chemical modification, it is preferred to perform the chemical cross-linking with the ELRs themselves in aqueous solution.

The most essential prerequisite parameter for the clinical application of cross-linked polymer materials is their non-toxic properties. These properties depend on the biocompatibility of not only the polymer chains, but also the cross-linkers employed which often generate foreign molecules between polymer chains [25,32,33,37,38]. For instance, the cross-linkers (e.g., such as glutaraldehyde or hexamethylenediisocyanate) used for hydrogel formation may release toxic byproducts upon degradation or hydrolyzation of the oligomeric bridges [25,32,33,37,38]. In contrast, the water-soluble carbodiimide (e.g.,1-ethyl-3-(3--dimethylaminopropyl)-carbodiimide (EDAC)) is recognized as a non-toxic and biocompatible cross-linker [37–39]. Thus, it forms isopeptides without being incorporated itself as a part of the cross-linked structure, but is only converted into a water-soluble urea derivative of quite low cytotoxicity. For instance, cross-linking collagen and/or gelatin with EDAC has resulted in the generation of a biocompatible matrices in both in vitro and in vivo studies without significant toxicity, thus providing to allow good cell viability [37–40].

Performing this non-toxic reaction in the presence of cells to cross-link the biocompatible ELRs chains [10,12,14] using EDAC could pave the way for the development of biocompatible injectable hydrogels that can be used in a wide range of biomedical applications.

Overall, the activation of carboxylic groups of glutamic or aspartic acid to conjugate with amine groups of another amino acid through the carbodiimide-mediated amidation reaction is particularly attractive for biological applications. Up to now, the amidation reaction using the ELR-bearing carboxylic groups has not been addressed except for the work that examined the chemical modification with *p*-phenylazoaniline (azo-NH_2), 4[(2 amino)carbamoyl]-phenylboronic acid (FB–NH_2), polyethyleneglycol (PEG-NH_2) and 1-(β-hydroxyethyl)-3,3-dimethyl-6′-nitrospiro-(indoline-2,2′[2*H*-]benzopyran) (Sp-OH), but under anhydrous conditions in organic solvent to prevent the hydrolysis process [41–43]. Indeed, the chemical modification of carboxyl-containing macromolecules usually involves toxic organic solvents, as well as slow, complex and low-yield processes. This is associated with low coupling ratios even with reagent excess, due to the complexity of the molecule to be modified [41–44]. Apart from these studies, to the authors' knowledge, neither the chemical modification of these ELRs through amidation of the carboxylic groups, in aqueous solutions, nor their subsequent application to the formation of chemical hydrogels, have been addressed.

The main aim of the present work is to find a new and more efficient way to improve the cross-linking of ELRs chains in aqueous solutions in order to ensures the preservation of the self-assembly properties. Our paper provides significant innovation since it contributes with very good results (a high yield in the reaction is obtained) both to the chemical modification of ELRs and to the formation of biocompatible hydrogels. Under our experimental conditions, we have taken advantage of the ELR rational design from the point of view of the advantageous selection of the environment of the key chemical groups participating in the reaction. Thus, ELRs hydrogels with tunable viscoelastic properties are developed, using a simple, "*in-situ*", one-pot, fast and cost-effective process. This has been achieved by the well-known carbodiimide-mediated amidation reaction using a green, expeditious, and practically simple protocol for direct coupling of carboxyl with amine groups found on ELRs biopolymer chains under aqueous conditions. For this aim, two basic structural ELRs (Table 1) were synthesized (using recombinant DNA technology) and employed in order to analyze the possibility of efficiently carrying out one-pot modifications. Through rational design, the amino acid X in the penta-peptide sequence (VPGXG) has been substituted by V, I, E and K amino acids to generate ELRs with a well-controlled structure. The first ELR -called as E50I60 ELR (Table 1)- is composed of a hydrophilic (E50) and a hydrophobic block (I60), such that the hydrophilic block contains equally spaced carboxyl groups from glutamic amino acids along its chain. The second ELR - called as VKV24 ELR (Table 1)- contains equally spaced amine groups from lysine amino acids along its chain. Thus, the glutamic-rich E50I60 ELR will be interchain cross-linked "*in situ*" with the lysine-rich VKV24 ELR, in aqueous solutions, using water-soluble EDAC to promote the amidation

Table 1
Code name, amino-acid sequence and molecular weight ($M.W_t$) of the prepared ELRs.

ELR code	Amino-acid sequence	$M.W_t$ (Da)
E50I60	MESLLP–[((VPGVG)$_2$(VPGEG)(VPGVG)$_2$)$_{10}$]–(VGIPG)$_{60}$–V	46981
VKV24	MESLLP– [(VPGVG)$_3$(VPGKG)(VPGVG)$_2$]$_{24}$–V	60460

reaction. While the formed ELR chemical network would preserve the shape and elasticity of hydrogels, the self-assembly of the hydrophobic I60 block would be necessary to provide a tunable physical network to stimuli, such as temperature. To this end, the viscoelastic performance of the generated ELR chemical-physical network has been described.

2. Experimental and characterization methods

2.1. Construction, production and purification of E50I60 and VKV24 ELRs

Standard genetic engineering procedures were employed to generate the coding gene of ELRs with a fully controlled composition and chain length, as described elsewhere [13,16,20,45]. The coding gene of each monomer, based on the (VPGXG), X = G, E, I or K fragments, was encoded in a modified version of the cloning vector pDrive (Qiagen), known as pDAll. These fragments were flanked by two inverted Eam 1104 I (Ear I) and one Sap I restriction sites, which were used to introduce a controlled sequential concatenation of the gene segments by means of a recursive directional ligation (RDL) strategy. Thus, the desired multiblock-coding genes were constructed, and their sequences were examined by agarose gel electrophoresis and automated DNA sequencing. After that, each ELR gene was sub-cloned into a modified pET-25(+) expression vector and then transformed into the *E. coli* strain BLR (DE3) star (Invitrogen). Then, the *E. coli* expression colonies were ruptured, and the purification of ELRs was carried out by inverse transition cycling and characterized as described elsewhere [13,20,45]. Finally, ELRs were dialyzed against ultrapure water, lyophilized and stored at −20 °C.

2.2. Grafting of aniline molecules onto the E50I60 ELR chain

In order to detect the possibility of the carboxylic groups found along the E50I60 ELR to form amide bonds in aqueous solutions, the aniline molecule was first selected as an amine reagent. Thus, the E50I60 ELR (containing ten carboxyl groups along the recombinamer chain) was dissolved in ultrapure water at 50 mg/ml and at 4 °C (Fig. 1). Then, to 2 ml of E50I60 ELR solution, an equimolar amount of aniline reagent (1 eq, 2.76 mg), with respect to carboxyl groups, was added to the previous solution and mixed until dissolved at 4 °C. After that, an equimolar amount of EDAC (1 eq, 3.3 mg) was also added and mixed until dissolved at 4 °C. Then, the pH of the mixture was adjusted to about 5 at 4 °C. After that, the mixture was heated up to 37 °C for 1 h (h). Then, a white solid was appeared, and the mixture was centrifuged, and the precipitate was washed three times using ultrapure water. Finally, the precipitate was dissolved in ultrapure water at 4 °C, dialyzed against water and lyophilized. The obtained aniline-grafted E50I60 ELR was characterized using ^{1}H NMR and MALDI-ToF spectroscopies.

2.3. "In-situ" crosslinking of E50I60 ELR with VKV24 ELR using EDAC in aqueous solutions

The E50I60 ELR was dissolved in ultrapure water at 50 mg/ml in an Eppendorf at 4 °C. Also, the VKV24 ELR was dissolved in ultrapure water at 50 mg/ml in another Eppendorf at 4 °C. After that, 349 μl of 50 mg/ml VKV24 aqueous solution is brought together with 651 μl of 50 mg/ml E50I60 ELR aqueous solution in such a way that the number of NH_2 moles equals the number of COOH moles in the final mixture solution at 4 °C (see Table 2 for quantities) (Fig. 2a). After that, the mixture was adjusted to a pH of about 5. This mixture is called as 50 EK, which contains a concentration of 50 mg/ml of the ELRs in the aqueous solution (Table 2). Then, an equimolar amount of EDAC (1 eq, 1.33 mg), with respect to carboxyl groups, was added to the 50 EK mixture at 4 °C, and the pH was again adjusted to about 5 at 4 °C. Finally, this sample was incubated in a mold at 37 °C for 1 h until the hydrogel was formed. The mold-formed hydrogel at a concentration of 50 mg/ml is called as

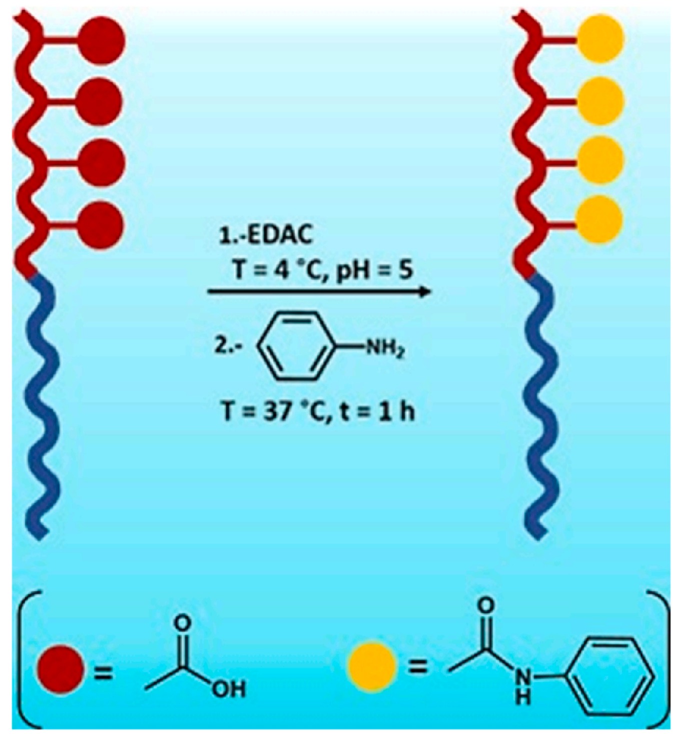

Fig. 1. Schematic representation of the reaction between –COOH groups from E50I60 ELR chains and –NH_2 groups from the aniline molecules through the carbodiimide-mediated amidation reaction; E50 and I60 blocks are represented by red and blue colour, respectively.

Table 2
Code name of the prepared ELRs mixtures with and without EDAC. A, B and C are 50, 100 and 150 mg/ml of E50I60 aqueous solutions, respectively, and D, E and F are 50, 100 and 150 mg/ml of VKV24 aqueous solutions, respectively.

Sample code	Description	Concentration of ELR
50 EK	651 μl of A + 349 μl of D	50 mg/ml (32.55 mg of E50I60 + 17.45 mg of VKV24)
100 EK	651 μl of B + 349 μl of E	100 mg/ml (65.11 mg of E50I60 + 34.89 mg of VKV24)
150 EK	651 μl of C + 349 μl of F	150 mg/ml (97.66 mg of E50I60 + 52.34 mg of VKV24)
50EKG	651 μl of A + 349 μl of D + 1.33 mg of EDAC	50 mg/ml (32.55 mg of E50I60 + 17.45 mg of VKV24)
100EKG	651 μl of B + 349 μl of E + 2.66 mg of EDAC	100 mg/ml (65.11 mg of E50I60 + 34.89 mg of VKV24)
150EKG	651 μl of C + 349 μl of F + 3.98 mg of EDAC	150 mg/ml (97.66 mg of E50I60 + 52.34 mg of VKV24)

50EKG. Similarly, the hydrogel formation was performed both from 100 mg/ml E50I60 & 100 mg/ml VKV24 and 150 mg/ml E50I60 & 150 mg/ml VKV24 aqueous solutions (Table 2). Thus, the aqueous mixture prepared from the 100 mg/ml E50I60 and 100 mg/ml VKV24 is called as 100 EK, and the mold-formed hydrogel is called as 100EKG. Also, the aqueous mixture prepared from 150 mg/ml E50I60 and 150 mg/ml VKV24 is called as 150 EK, and the mold-formed hydrogel is called as 150EKG (Table 2).

2.4. Characterization techniques

Matrix-assisted laser desorption/ionization time-of-flight (MALDI-TOF) mass spectrometer was used to record the mass spectra of the E50I60 ELR with the aniline grafts. The employed matrix was a mixture of dissolved 2,5-DHAP (7.6 mg) in ethanol (375 μL) and 125 μL of 18

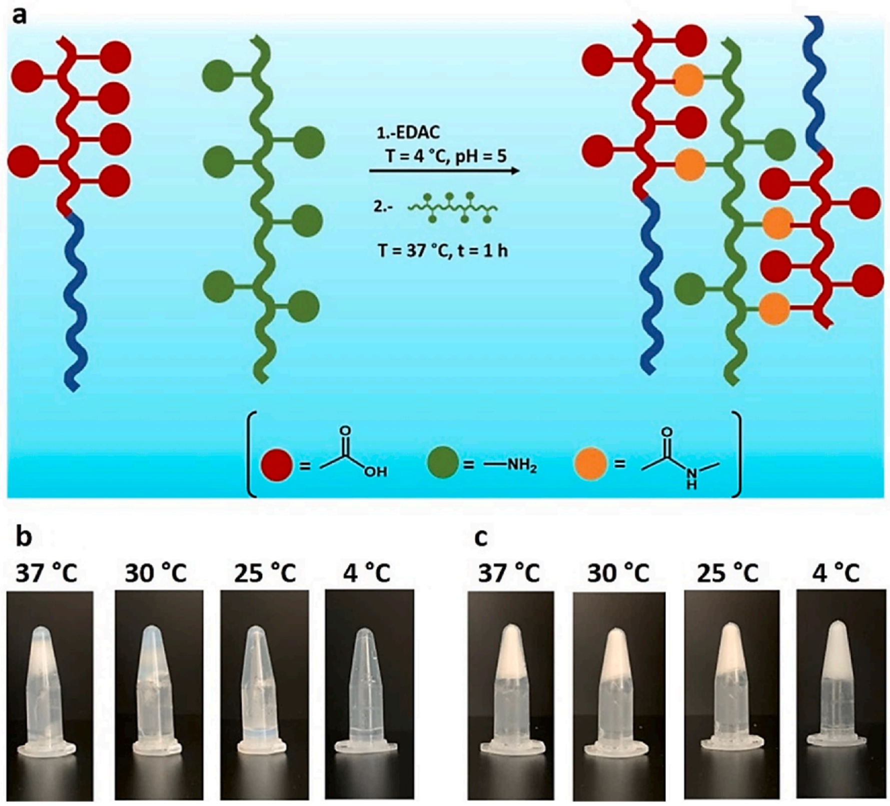

Fig. 2. (a) Schematic representation of the reaction between –COOH groups from E50I60 ELR chains and $–NH_2$ groups from VKV24 recombinamer through the carbodiimide-mediated amidation reaction; VKV24, E50 and I60 blocks are represented by green, red and blue colour, respectively. Photographs of the (b) 50 EK, and (c) 50 EK + EDAC (1 eq) mixtures after incubation at 37 °C for 1 h and at different temperatures. This figure shows a macroscopic test to clarify the irreversibility of the hydrogel formation when the temperature decreases from 37 °C to 4 °C (Fig. 2c) in contrast with reversible coacervate formation in the absence of EDAC (Fig. 2b).

mg/mL $C_6H_8O_7{\cdot}2NH_3$ aqueous solution. Then, 1 μL of this mixture was introduced along with 1 μL ELR aqueous solution (1 mg/ml) to the MALDI plate. Finally, the mass spectra were recorded for the dried plate by using a Bruker autoflex speed instrument equipped with a nitrogen laser (337 nm).

NMR spectra were recorded using 500 MHz Agilent DD2 instruments equipped with a cold probe in the Laboratory of Instrumental Techniques (LTI) Research Facilities, University of Valladolid. ^{1}H NMR spectra of the E50I60 ELR with aniline grafts was carried out at 298 K with the dissolved modified-ELR sample at concentration 25 mg/ml and for 650 μl of D_2O. ^{1}H chemical shifts (δ) are reported in parts per million (ppm). In order to obtain a quantitative ^{1}H NMR spectrum the acquisition parameters were:10 s relaxation delay between transients, 45° pulse width, spectral width of 8012 Hz, a total of 16 transients and 2.044 s acquisition time.

Differential scanning calorimetry (DSC) analysis was performed using a Mettler Toledo 822e. The measurements were carried out in the range of 5–60 °C, and at a heating rate of 5 °C/min. Thus, 20 μL of the prepared E50I60, VKV24 and 50 EK ELR solutions (at a concentration of 50 mg/ml in ultrapure water, with and without the addition of EDAC (1eq), at a pH of about 5) were placed in a 40 μL sealed aluminum pan, and the same volume of ultrapure water was placed in the reference pan.

In order to study the microstructure of the prepared ELR hydrogels, the incubated ELR hydrogel at 37 °C was rapidly immersed in liquid nitrogen, fractured mechanically using tweezers, and then lyophilized. Thus, the lyophilized sample was metalized with gold to take the SEM micrographs in low-vacuum mode with water as the auxiliary gas, using the FEI Quanta Field Emission Scanning Electron Microscopy (SEM). The average pore size was determined using the Digital Micrograph software, by quantifying the size of at least 20 pores. Furthermore, the lyophilized hydrogel samples were fixed on a glass substrate to study the topographical structure, using a Witec atomic force microscopy (AFM) in the tapping (AC) mode with a Si_3N_4 Cantilever (spring constant k = 2.8 N/m, WITec, Ulm, Germany) and the 20x objective (NA = 0.5, Olympus, Japan). Rheological dynamic experiments were performed using a stress-controlled AR-2000ex rheometer (TA Instruments) using a parallel plate geometry and equipped with a Peltier accessory to control and maintain the sample temperature. Several measurements were accomplished, and then, the evolution of the storage (G′) and the loss (G″) moduli on temperature, strain and frequency were obtained for three different sample concentrations (50, 100 and 150 mg/ml). In the case of temperature and frequency sweeps, a strain of 0.3% was used. In every measurement, a gap larger than 1000 μm was always used. Solutions of 50 EK, 100 EK or 150 EK, with and without the addition of EDAC (1eq), at 4 °C were injected directly between the 20 mm parallel plates. In order to analyze the *"in-situ"* gelation on the rheometer plate, a temperature sweep (at a fixed frequency of 1 Hz) was carried out from 5 to 50 °C (the heating cycle) and from 50 to 5 °C (the cooling cycle) at the same constant rate of 2 °C/min; the cooling cycle immediately followed the heating cycle. A solvent trap accessory was used to maintain sample humidity, preventing the sample from drying out. As for 50EKG, 100EKG and 150EKG samples, strain and frequency sweeps at 4 or 37 °C were carried out on cylindrical gel samples (φ = 12 mm) using a 12 mm diameter rheometer plate. These three samples were measured in rheology immediately after the incubation time (1 h) was over. Rheological measurements provide the storage modulus (G′) and the loss modulus (G″) as a function of strain or frequency at a fixed temperature. The complex modulus magnitude $|G^*|$ ($|G^*|^2 = (G')^2 + (G'')^2$), and the loss factor tan δ (tan $\delta = G''/G'$, where δ is the phase angle between the applied stimulus and the corresponding response) was also obtained. Each sample was measured in triplicate, and the values are reported as the mean and standard deviation.

3. Results

In this section, the design and bioproduction of the ELRs, their modification and subsequent hydrogel formation by means of the carbodiimide-mediated amidation reaction are described. Furthermore, an exhaustive characterization of the proposed new material has been carried out by means of different experimental techniques, such as DSC, rheology, SEM and AFM. The correlation of all these techniques and the global discussion has allowed us to propose, finally, a tentative mechanism for the formed hydrogel tunable viscoelasticity.

3.1. ELRs construction, production and purification

The combination of various polypeptide domains inspired by proteins in a single polymer chain is the key to generating biomimetic materials with intricate complex structures and the desired functional properties [13,20,36,45,46]. This can be successfully produced with a fully controlled composition and appropriate chain length through standard genetic engineering procedures. For instance, the corresponding coding gene of (VPGXG), where X = G, E, I or K, amino acid fragments can be consecutively introduced through the recursive directional ligation (RDL) technique to construct the gene of the amphiphilic E50I60 or VKV24 ELRs. DNA sequencing has demonstrated the accuracy of gene construction and, therefore, the desired ELRs have been produced. By means of their inverse temperature transition, the E50I60 or VKV24 ELRs were purified and, subsequently, characterized as previously determined [13,20,45]. While the E50 hydrophilic block of the E50I60 ELR contains ten equally spaced carboxylic (–COOH) groups from glutamic amino acids along its chain, the VKV24 ELR contains twenty-four equally spaced amines (–NH_2) groups from lysine amino acids along its chain. Thus, the –COOH groups from glutamic acid (E) can undergo a reaction to form amide bonds with amine reagents through the carbodiimide-mediated amidation reaction.

3.2. Conjugation of the aniline molecule with E50I60 ELR

It has been claimed that the chemical modification of the carboxylic groups present along an ELR polymer chain is usually a slow, complex and low-yield process, with a moderate coupling ratio, that requires the previous activation of the carboxyl group [41–43]. That is the main reason why, in general, the chemical modifications of ELRs have been carried out on recombinamers designed to have the amino groups of the lysines along their chain [20,34–36]. Our first objective in this work, therefore, would be to test the reactivity of the carboxyl groups present in E50I60 ELR upon amidation modification. We chose aniline as the standard amine to carry out the amidation tests prior to optimization of the modification method. Aniline contains one NH_2 group and, thus, the ten carboxylic groups found along the E50I60 ELR are able to react at maximum with ten aniline molecules, giving rise to the conjugated E50I60 chains with aniline molecules (Fig. 1).

Overall, the amidation reaction of E50I60 in aqueous medium was carried out in the presence of equimolar amounts of EDAC, equimolar aniline, and at the physiological temperature. The E50I60 and aniline molecules were mixed in an aqueous solution with the addition of EDAC in order to allow insufficient time for the unstable intermediate O-acylisourea to hydrolyze before amide bonds were formed with the NH_2 groups. Aniline was also chosen as an amine reagent because it has an aromatic structure, whose protons resonate at different fields from the protons present in the ELR to be modified. So, the conjugation of the aniline molecules to the ELR was corroborated through the study of their structure by means of their ^1H NMR spectrum in D_2O (Figures S1a–1b).

Figure S1b displays the appearance of new and characteristic signals of aromatic protons at 6.7–7.7 ppm in the E50I60 ELR conjugated with aniline molecules, which are not present in the unmodified E50I60 ELR spectrum (Figure S1a). These signals are attributed to the aromatic protons of the aniline molecule. From the analysis of the integrals of these aromatic protons, it is deduced that a total of seven aniline molecules have been conjugated. Furthermore, MALDI-ToF mass spectra display the increase in molecular weight attributed to the same aniline conjugation to E50I60 (Figure S1c). It should be noted that we have demonstrated, both by NMR and MALDI-ToF, that a conversion of about 70% has been obtained. Therefore, the carbodiimide-mediated amidation reaction successfully demonstrates to be achievable in a simple and highly efficient process in the aqueous phase for our materials. This fact motivates us to produce a hydrogel with the participation of both the ELRs bearing COOH groups and the ELRs bearing NH_2 groups with the same amidation procedure for chemical crosslinking of the chains.

3.3. Crosslinking of E50I60 ELR and VKV24 ELR: thermodynamic characterization

In view of the above results, we applied the aforementioned methodology to the chemical chain cross-linking of E50I60 ELR with another biopolymer that contains sparsely distributed amine groups in its structure, such as VKV24, in order to generate a hydrogel matrix. As the VKV24 contains about twenty-four amine groups, the addition of EDAC can result in a cross-linked matrix (in the insoluble state). In this regard, the "*in-situ*" hydrogel quantitative studies by DSC and temperature sweep rheology analyses will be employed for their characterization.

Fig. 2a shows the schematic representation of the reaction between –COOH groups from E50I60 ELR chains with –NH_2 groups from the VKV24 recombinamer through the carbodiimide-mediated amidation reaction in one-pot step approach. For instance, this can be visually observed when the 50 EK aqueous solution is mixed without and with EDAC (1eq) (Fig. 2b and c, respectively). Fig. 2b shows that the photographs of 50 EK (without the addition of EDAC) at 37 °C present the exclusion of an amount of water from the 50 EK mixture. This indicates that 50 EK at 37 °C just forms a phase-separated state as the I60 blocks in the E50I60 ELR chains have the ability to assemble with each other through the hydrophobic interactions and form an aggregated state [13,22,23]. With decreasing the temperature from 37 to 4 °C, these aggregations are gradually solubilized in the aqueous solution, as the temperature goes below the intrinsic T_t (19 °C) value [13] of the I60 blocks. In other words, the I60 blocks are transformed from ordered to a disordered state. On the contrary, Fig. 2c shows that the addition of EDAC (1 eq) to 50 EK results in the rapidly formation of a hydrogel matrix at 37 °C, which is irreversible when cooled again from 37 to 4 °C; this irreversible behavior indicates the presence of a chemically cross-linked hydrogel.

3.4. DSC thermograms of E50I60 and/or VKV24 without and with the addition of EDAC

As the ELRs chains exhibit self-assembly properties dependent on their transition from disordered to ordered states [20,34–36], the effect of EDAC molecules and/or VKV24 ELR on the T_t of E50I60 has been studied by DSC. Fig. 3 shows that there are endothermic peaks, which are characterized by the peak temperature (T_t, transition temperature by DSC) at about 18.5 and 43.6 °C for E50I60 and VKV24 ELRs, and enthalpies (ΔHs) involved in this transition of about 8.6 and 2.1 J/g (Table 3), respectively. The decrease in T_ts with the EDAC (1 eq) addition to E50I60 or VKV24 ELRs indicates that EDAC molecules enhance the folding and aggregation processes of the ELRs chains. Furthermore, ΔHs increases to about 11.2 and 3.7 J/g, respectively. When the E50I60 and VKV24 ELRs are mixed (e.g., 50 EK) in ultrapure water, both T_ts are observed in the corresponding thermogram, but that corresponding to the VKV24 ELRs shifts to a lower temperature (~39.8 °C), whereas the T_t corresponding to the E50I60 ELRs is not affected. This decrease could be attributed to the electrostatic interaction between –NH_3^+ and –COO^- groups, thus increasing the transition of ELRs chains from disordered to ordered structures. This means that E50I60 can also affect the self-assembly properties of VKV24, thus giving rise to a phase-separated

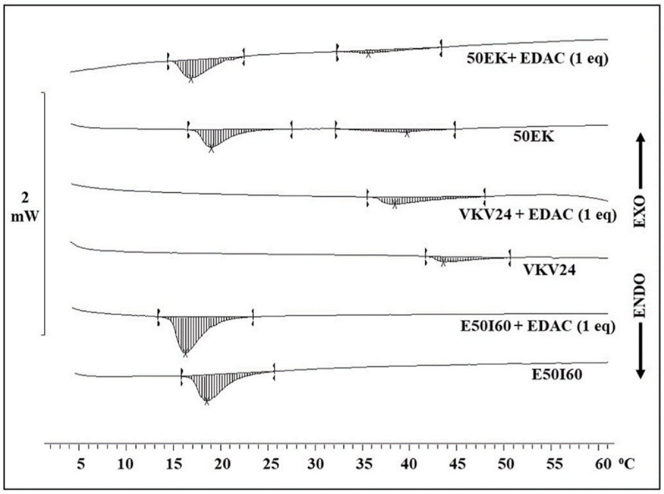

Fig. 3. DSC thermograms of E50I60, VKV24 and 50 EK in aqueous solution without and with the addition of EDAC (1 eq).

Table 3
T_t, transition temperature by DSC, and enthalpy, ΔH, of E50I60, VKV24 and 50 EK in aqueous solution without and with the addition of EDAC.

Sample code	T_t (°C)		ΔH (J/g)	
	(E50I60)	(VKV24)	(E50I60)	(VKV24)
E50I60	18.5		8.6	
E50I60 + EDAC (1 eq)	16.3		11.2	
VKV24		43.6		2.1
VKV24 + EDAC (1 eq)		38.4		3.7
50 EK	19.0	39.8	5.7	1.9
50 EK + EDAC (1 eq)	16.9	35.7	6.1	1.2

state at 37 °C as the ELR chains are aggregating with each other (Fig. 2b). Again, the addition of EDAC molecules to the mixture of E50I60 with VKV24 (i.e., 50EKG) causes a further reduction in T_ts to ~ 16.9 and 35.7 °C, respectively, in the same proportion as for each ELR separately (Fig. 3). This result, together with the irreversible hydrogel obtained in Fig. 2c, allows us to suggest that this reduction might be attributed to the chain chemical cross-linking caused by the formation of amide bonds between ELR molecules.

3.5. *ELR hydrogel formation mechanism: tunable viscoelasticity with temperature*

As the E50I60 ELR can self-assemble into a physical hydrogel [13], the effect of the presence of VKV24 on the moduli of the self-assembled E50I60 ELR hydrogel has been studied through a rheometer temperature sweep analysis in order to accomplish an "*in situ*" gelation on the rheometer plate. Figure S2a–2b shows that 50 EK and 100 EK mixtures (without the addition of EDAC (1eq)) result in very low values of G′ and G″, thus indicating that the system remained in a liquid state and no gelation occurred. Indeed, it has been demonstrated that E50I60 at 50 and 100 mg/ml can form a physically cross-linked network with a gelation temperature (T_{gel}) of ~33 and 21 °C, respectively, and G′ moduli of about 1088 and 3197 Pa, respectively [13]. In contrast, no gelation takes place with the addition of VKV24 (as in 50 EK and 100 EK: Figures S2a–2b). Even for higher concentrations of both ELRs (as in 150 EK) the formation of an unstable, reversible hydrogel (Figure S2c), has resulted in high T_{gel} (45 °C) and low G′ values (300 Pa), as compared to that of 100 mg/ml E50I60 (33 °C, 3197 Pa) [13]. This demonstrates that VKV24 addition affects the self-assembly properties of the E50I60 ELR chain.

The cross-linking of E50I60 with VKV24 ELRs chains by means of the amidation reaction can be followed through monitoring the rheometer temperature sweep (heating and cooling cycles) analysis at a constant frequency. Fig. 4 shows the temperature sweep of 50 EK, 100 EK and 150 EK after the addition of EDAC (1 eq). The most obvious finding is the different evolution of the elastic modulus (G′) and the loss (viscous) modulus (G″) as compared to that of the 50 EK, 100 EK and 150 EK mixtures without the addition of EDAC (1eq) (Figure S2). Thus, Fig. 4a–c shows that G′ and G″ display a rapid increase in both magnitudes at a certain temperature; a sigmoidal evolution is observed for the lowest concentration. When temperature increases, a crossover point between G′ and G″ is observed. The temperature at which G′ = G″ is defined as the T_{gel} (at the selected frequency: 1 Hz in this case) measured by rheology [13,47–49]. Indeed, the value of T_{gel} depends on the concentration of ELR in aqueous solution, which decreases from ~29 to 26 or to 16 °C as the concentration of the mixed ELRs (E50I60+VKV24) is increased from 50 to 100 or to 150 mg/ml, respectively (see Fig. 4a–c). Above the T_{gel}, the increasing behavior in G′ and G″ moduli are dependent on the ELR concentration, and G′ was larger than G″, corresponding to the hydrogel formation. For instance, at 41 °C, whereas G′ and G″ are ~50 and 6 Pa, respectively, for 50 EK, these moduli are ~1043 and 132 Pa, respectively, for 100 EK, and are about 1190 Pa and 276 Pa, respectively, for 150 EK.

Focusing our attention on the elastic modulus, Fig. 4d shows that G′ displays the presence of two plateaus. A high-temperature plateau is observed in all concentrations above 29 °C. In this region, G′ is about 50, 1043 and 1190 Pa for 50 EK, 100 EK and 150 EK, respectively. A low-temperature plateau between 10 and 29 °C is observed for 100 EK by the change in the slope of G′ and G″ and clearly seen for 150 EK. At the end of the heating cycle, the hydrogel is formed, and immediately after that the cooling cycle (Figure S3) starts. At 37 °C ELR chains are contracted, while at 4 °C these chains are extended, giving rise to the corresponding change in moduli values. The evolution of these moduli with temperature shown in this figure quantitatively indicates the presence of the irreversible amide (chemical) bond.

3.6. Dynamic dependence of hydrogel viscoelasticity:

The rheological hydrogel characterization was completed with frequency response measurements. In this regard, each hydrogel was tested over its respective linear viscoelastic range in order to study the impact of frequency on G′ and G″ of the formed 50EKG, 100EKG and 150EKG hydrogels. |G*| was found to remain independent of strain (linear viscoelastic behavior) up to values of about 3% (see Figure S4). Thus, the measurements were carried out within the linear viscoelastic region, at 0.3% strain as a trade-off between linearity and noise in measurements. Fig. 5a–c shows the frequency dependence of G′ and G″ at 4 °C for the mold-prepared ELRs hydrogels. The values of both G′ and G″ increase with frequency. Furthermore, the elastic G′ modulus for all hydrogels is larger than its corresponding viscous modulus G″, indicating that a stable gel state was formed. Whereas a low frequency-dependence of G′ values is found in the range from 0.01 to 2 Hz for 50EKG, a certain evolution is observed when concentration increases (100EKG, and 150EKG). Indeed, the G′ values of 50EKG, 100EKG and 150EKG at 4 °C remain in the same order of magnitude. For instance, the values at 1 Hz of G′ for 50EKG, 100EKG and 150EKG hydrogels are about 257, 430 and 472 Pa at 4 °C. This is attributed to the disruption of the interchain hydrophobic contacts between the ELR chains, which are extended and tend to be hydrated with water molecules. As far as G'' is concerned, the trend to increase with frequency is similar for the three concentrations, but its value shows a slight increase with concentration.

Fig. 5d–f shows the dependence of G′ and G″ at 37 °C. As can be seen, while G′ monotonically increases when frequency does for each concentration, G'' shows a dip in the frequency range of 0.2–10 Hz where this modulus falls and rises; its depth is higher for the highest concentration. At 37 °C similar G′ values are found for 100 EK and 150 EK, whereas G'' values show a slight increase with concentration. Both G′ and G'' are significantly lower for the lowest concentration considered (50 EK). Furthermore, the frequency dependence of the G′ modulus is

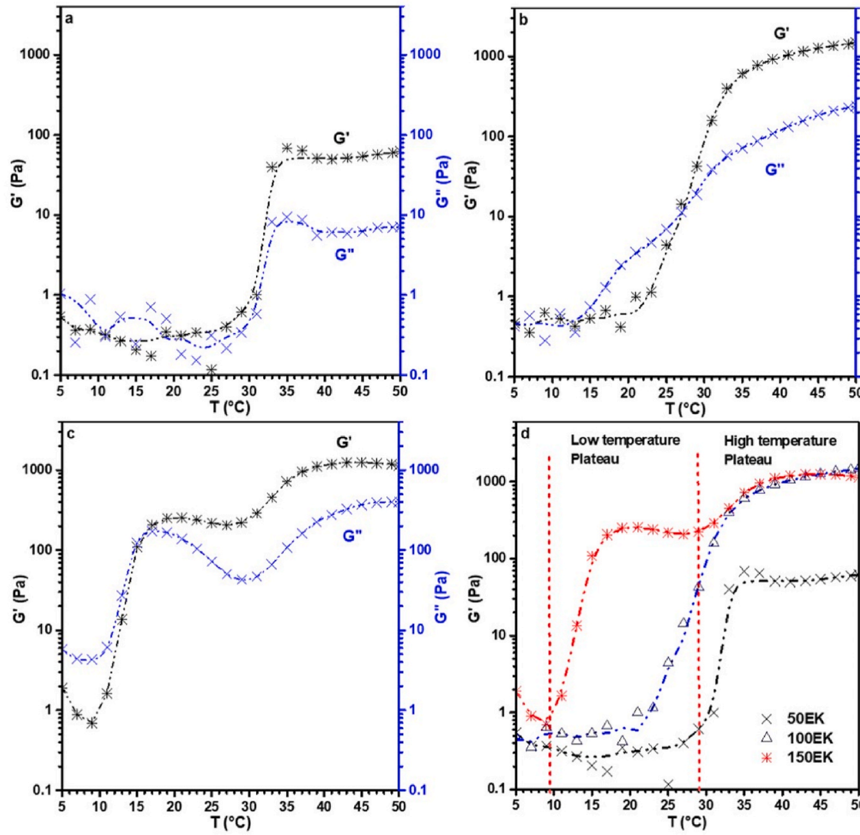

Fig. 4. Temperature dependence of G′ and G″ moduli as the temperature increases from 5 to 50 °C (heating cycle) for (a) 50 EK, (b) 100 EK and (c) 150 EK, with the addition of EDAC (1eq). d) Evolution of the G′ modulus for the three concentrations throughout the low and high temperature plateau regions, which are indicated by the dashed red lines.

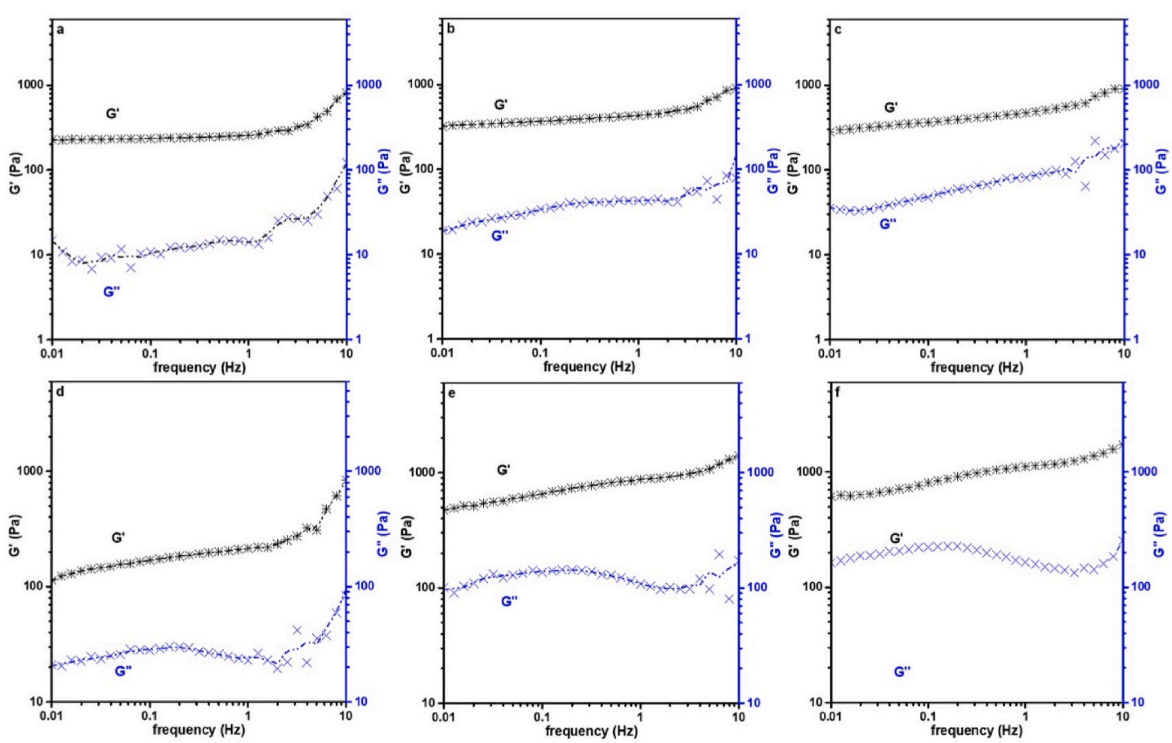

Fig. 5. Frequency dependence of the storage, G′ and loss, G″ moduli for: (a) 50EKG, (b) 100EKG, and (c) 150EKG at 4 °C; (d) 50EKG, (e) 100EKG and (f) 150EKG at 37 °C.

affected by temperature. Focusing our attention on G′ at 1 Hz, while relatively similar values are obtained for the three concentrations at 4 °C, a clear increase is found at 37 °C (Table 4). The transition of the I60 blocks (with a T_t of about 19 °C) from disordered to ordered states as the temperature changes from 4 to 37 °C, through the interchain hydrophobic contacts and forms a physical network structure contributes to the G′ increase. This network structure tends to be hydrated with water molecules and extended as the temperature changes from 37 to 4 °C.

Concerning the loss factor (Figure S5), a different evolution is observed at 4° and 37 °C. Whereas at low temperatures this parameter tends to increase for each concentration throughout all the frequency ranges considered, at 37 °C tan δ shows the behavior corresponding to G'′, reaching a minimum at 7–8 Hz (tan $\delta \approx 0.1$, $\delta \approx 5$–6°) for the three concentrations where the elastic behavior of the hydrogel is maximized. At low frequencies, higher values of tan δ are found at 37 °C than at 4 °C, indicating again the higher hydration of the ELR chains at low temperatures. The hydrogels are contracted at 37 °C and therefore have a lower water content, meaning that less water is available to lubricate chain reorientation in response to an applied strain. Additionally, the ELR chains are able to withstand extensive interchain hydrophobic contacts at temperatures above the characteristic phase transition temperature.

In Fig. 6a–b, the dependence of the complex modulus magnitude, |G*|, with $f^{1/2}$ has been plotted in order to obtain a deep insight into the physical mechanism that determines the frequency evolution of the hydrogels at 37 and 4 °C, respectively. At the lowest frequencies, a non-linear dependence of |G*| with $f^{1/2}$ is found, and at 37 °C its corresponding frequency range is more extended when concentration increases. This region corresponds to the intrinsic viscoelasticity, where a fluid-independent viscoelastic mechanism dominates, such as relaxation, reconfiguration and conformational mobility of recombinamer chains [20]. As can be seen in this figure, a region with a linear dependence of |G*| with $f^{1/2}$ is also observed where a poroelasticity (fluid-dependent) mechanism dominates, involving that viscous drag of interstitial fluid (water) through the porous recombinamer network and fluid-solid frictional interactions associated to fluid pressurization prevail. The slope of this linear region is related to hydrogel permeability, or in other words, the ease with which a fluid flows through the hydrogel matrix [20]. The frequency range where this mechanism dominates is considerably more extended at 4 °C than at 37 °C, and for a given temperature, it is reduced when concentration increases.

In Fig. 6c, the slope of this region has been drawn; the slope increase is observed when concentration increases, thus corresponding to a decrease in the hydrogel permeability. The values found in our hydrogels are in the same order of magnitude of those obtained in ELR click gels [20] and hybrid ELR-fibrins [50] based on chemical crosslinking. For a given concentration, a higher slope is calculated at 37 °C than at 4 °C, corresponding to a higher permeability at low temperatures. At a fixed temperature, the higher the slope, the lower the hydrogel permeability.

Table 4
Elastic (G′) and loss moduli (G″) and phase angle, δ, at 1 Hz of 50EKG, 100EKG and 150EKG at 4 and 37 °C.

	4 °C			37 °C		
	G′ (Pa)	G″ (Pa)	δ (degrees)	G′ (Pa)	G″ (Pa)	δ (degrees)
50EKG	257 ± 12.9	14 ± 0.7	3.2 ± 0.2	215 ± 10.8	24 ± 1.2	6.1 ± 0.3
100EKG	430 ± 21.5	43 ± 2.2	5.7 ± 0.3	874 ± 43.7	109 ± 5.5	7.1 ± 0.4
150EKG	472 ± 23.6	83 ± 4.2	9.8 ± 0.5	1115 ± 55.8	166 ± 8.3	8.5 ± 0.4

3.6. Morphological characterization of the hydrogel

The previous rheological results about gel permeability were confirmed by the following morphological characterization based on SEM. In this regard, the formation of a reliable pore structure within the network of 50EKG, 100EKG and 150EKG at 37 °C has been observed using the SEM micrographs. Fig. 7 shows that the internal structure of the prepared hydrogels displays a homogeneous porous structure with high interconnectivity. As the ELR concentration increases from 50 to 150 mg/ml, the structure becomes denser and more compact, and therefore, the pore size decreases in agreement with the rheological results shown in Fig. 6c [20], since permeability increases when porosity does [51]. Thus, the SEM micrographs (Fig. 7) displays that the pore size decreases from 3.9 ± 1.3, 2.6 ± 0.9 and 1.3 ± 0.5 μm as the concentration increases from 50, 100 and 150 mg/ml, respectively.

Fig. 8 presents the AFM micrographs of the prepared hydrogel matrix. In Fig. 8d–f, a higher magnification of the areas indicated in Fig. 8 a-c have been included. Fig. 8d (50EKG) shows the presence of three dimensional nanostructures, whose linear dimension dominates (focusing on the greatest nanostructure: length close to 2 μm, thickness around 250 nm) along with some spherical or semispherical nanostructures (with diameter of about 50–100 nm). In Fig. 8e and f, 100EKG and 150EKG exhibit the presence of semispherical nanostructures dominates (with a diameter of about 100–200 and 250–400 nm, respectively) in a higher amount than in Fig. 8d.

4. Discussion

ELRs have demonstrated their significance in the generation of physically or chemically cross-linked hydrogels. On one hand, ELRs chains can be well-constructed through the recombinant DNA technology in order to exhibit physical cross-linking through hydrophobic interactions. For instance, it can be found in the bibliography that the E50I60 ELR in aqueous solution exhibits controllable thermoresponsive behavior [13,19,45]. Above its T_t (19 °C), the E50I60 chains interact with each other, giving rise to micellar structures, such that I60 blocks interact with each other through hydrophobic interactions to form the core while the hydrophilic E50 blocks form the corona. These nanoparticles can be organized with each other into physical hydrogels. It has been demonstrated that E50I60 at 50 and 100 mg/ml can form a physically cross-linked network with a gelation temperature (T_{gel}) of ~33 and 21 °C, respectively, and G′ moduli of about 1088 and 3197 Pa, respectively (see Fig. 5a from Ref. [13]). However, the formed physical hydrogel is still reversible when placed below the intrinsic T_t of E50I60 ELR. In this work, we have proved that the addition of VKV24 ELR bearing positively charged amine groups to the E50I60 bearing negatively charged carboxylic groups has resulted in very low values of G′ and G″ (Figures S2a-2c). Thus, no gelation takes place above the T_t, and it may have a lot to do with electrostatic interactions between the opposite electric charges of $-NH_3^+$ and $-COO^-$ groups found on the VKV24 and E50I60 ELRs, respectively. This electrostatic interaction is demonstrated by lowering the T_t of VKV24 ELRs to ~39.8 °C (50 EK), and a certain amount of water is excluded from the aqueous ELR mixture to generate a phase-separated state (see Fig. 2b) rather than the formation of a physical hydrogel. Overall, the mechanical strength above the intrinsic T_t of ELR due to the physical cross-linking of ELR chains through the hydrophobic and/or electrostatic interactions is extremely limited.

On the other hand, ELRs chains can be successfully generated through the proper molecular design to bear the appropriate functional groups, such as amine or carboxylic groups, for further chemical modification. Indeed, it can be found that the ELRs chemical modifications could be carried out through the functionalization of amino groups of the lysines, for example, with azido and cyclooctyne groups [20, 34–36]. Thus, the ELRs chains (e.g., VKV24) can be chemically cross-linked by means of catalyst-free click chemistry (azide−alkyne [3

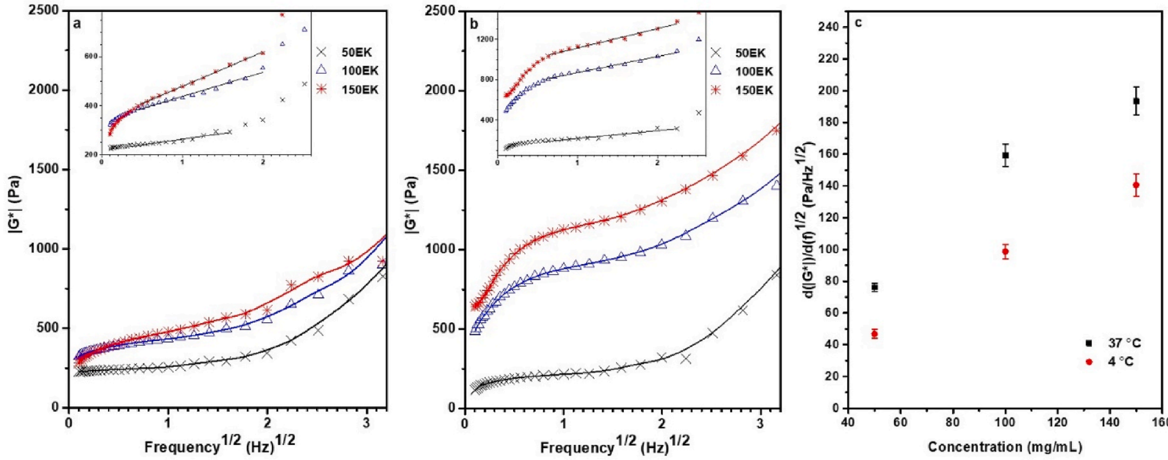

Fig. 6. Dependence of |G*| on square root of frequency ($f^{½}$), at 4 °C (a) and 37 °C (b), for 50 EK (50 mg/ml), 100 EK (150 mg/ml) and 150 EK (150 mg/ml). (c) d(|G*|)/d($f^{½}$) for 50 EK (50 mg/ml), 100 EK (150 mg/ml) and 150 EK (150 mg/ml) hydrogels, at 4 and 37 °C. In figures (a) and (b), the insert includes a zoom of the frequency region where the linear dependence between |G*| on $f^{½}$ takes place; in these inserts, the axis and units are the same as in the main figure.

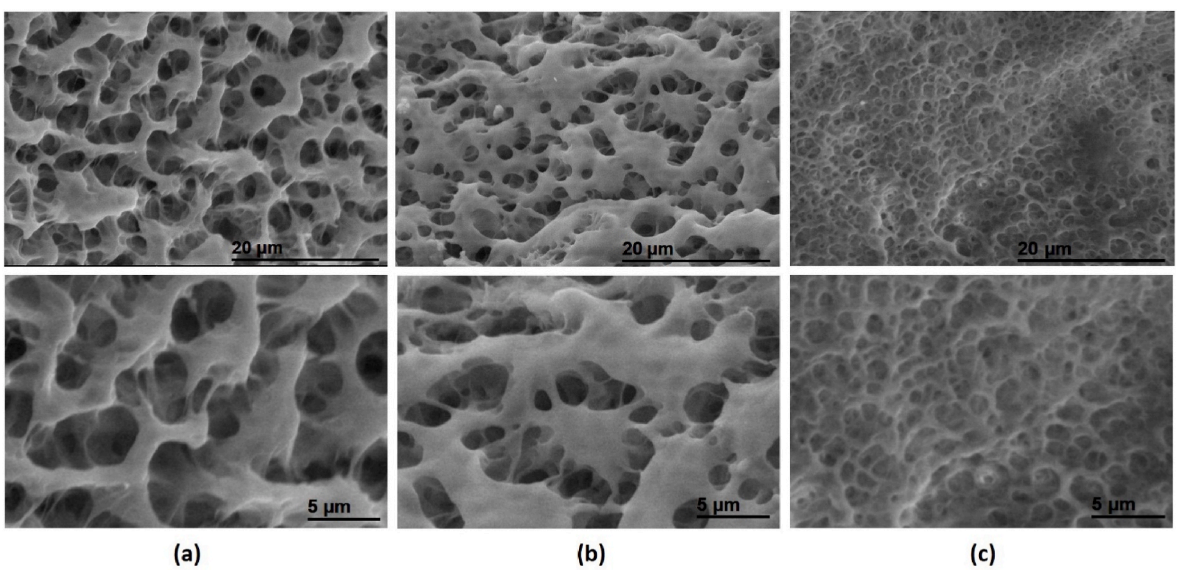

Fig. 7. SEM micrographs of (a) 50EKG, (b) 100EKG and (c)150EKG hydrogels at 37 °C. A higher magnification has been used for each micrograph in the bottom row.

+ 2] cycloaddition) [20,34,52,53]. This resulted in a hydrogels structure with a G′ of about 1.8 kPa–7.5 kPa as the concentration increases from 50 to about 150 mg/ml. In contrast, chemical modification of ELRs through the carboxylic groups present in their polymeric chain is usually a less efficient process with a moderate derivatization ratio, since it requires prior activation of the carboxyl group [41–43].

Amide linkages have demonstrated their significance in chemical cross-linking for various applications such as drug delivery systems (25% of all pharmaceutical products), wound healing and adhesives [54–60]. In conventional approach, the carboxylic acids are first activated, and the derivatives are followed by the nucleophilic attack of amino groups [58–60]. However, the synthesis process includes the use of expensive and/or toxic activators as well as organic solvents. In this regard, we have used the EDAC-mediated amidation method for the direct reaction of the carboxylic acid/amine pair of ELRs chains in a straightforward operational manner (Fig. 1). The success of this reaction is attributed to the electrostatic interaction between the opposite electric charges of the $–NH_3^+$ and $–COO^-$ groups found on the VKV24 and E50I60 ELRs, respectively. These interactions result in lowering the average polarity of the ELRs chains in the mixture (as demonstrated by DSC thermograms). Since the carboxylic and amine groups are close to each other through the electrostatic interactions, they are easily accessible for the amidation reaction upon the addition of EDAC. This mixing procedure aims to allow insufficient time for the unstable intermediate O-acylisourea to hydrolyze before amide bonds are formed with the NH_2 groups. Indeed, the present amidation process condition offers significant improvements in terms of safety and ease of setup with a high yield of amide linkages, as demonstrated by the previous amidation reaction of E50I60 carried out with an amine reagent such as aniline, which led to a 70% conversion of the carboxylic functional groups (Figure S1a–1b). Thus, this method is operationally simple, environmentally friendly, and operates in “industrially preferred” solvents under exceedingly mild conditions without the use of any additives or dehydrating agents, reducing its environmental impact.

The presence of two plateaus in the rheological study (Fig. 4) indicates that the gelation process is associated with a dual mechanism. In order to describe these experimental rheological results, it should be taken into account the concentration at which the amphiphilic E50I60 ELR can be physically cross-linked through the hydrophobic interactions and the decrease of T_t when the ELR concentration increases. Indeed, the

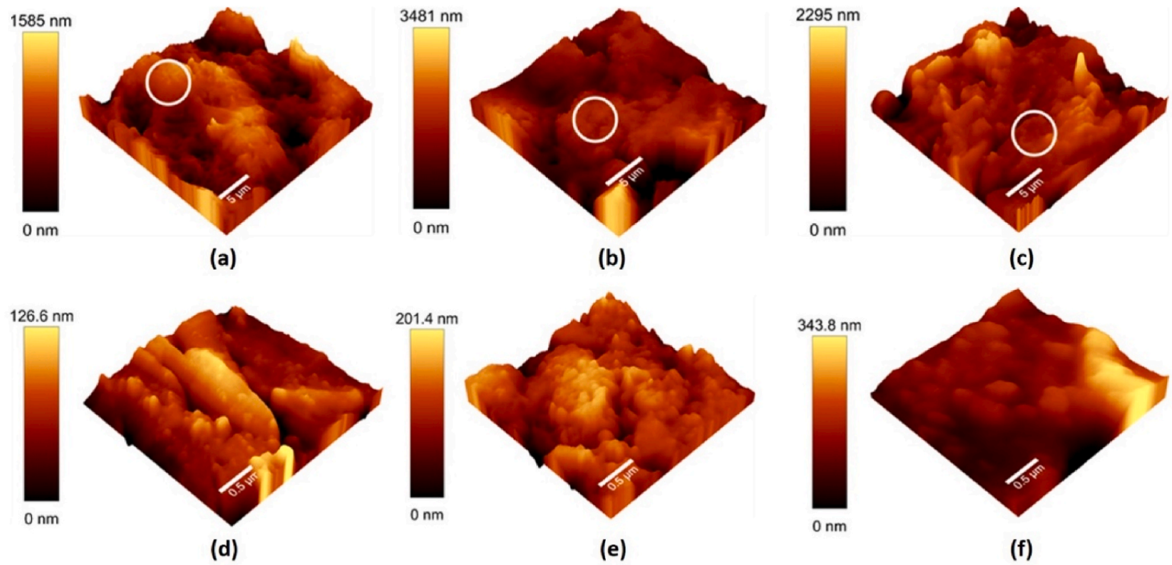

Fig. 8. AFM micrographs of 50EKG (a), 100EKG (b) and 150EKG (c) at a scanning area of 25 × 25 μm^2. The marked white circles have been scanned at an area of 2.5 × 2.5 μm^2 for 50EKG (d), 100EKG (e) and 150EKG (f).

concentration of E50I60 found in 50 EK solution is about 32.55 mg/ml (Table 2), which is not sufficient to form a physical hydrogel through the hydrophobic interactions [13,22,23]. This indicates that the *"in-situ"* formation of the 50 EK hydrogel is evidently due to the carbodiimide-mediated amidation reaction. On the contrary, the concentration of E50I60 found in 100 EK is about 65 mg/ml (Table 2), which is sufficient to aggregate through the hydrophobic interaction and form a physical hydrogel [13,22,23]. This indicates that the thermally driven self-assembly of the amphiphilic E50I60 ELR into the physical hydrogel network contributes to the G′ of 100 EK hydrogel. Although the change in the slope of G′ and G″ of 100 EK in the temperature range corresponding to the low temperature plateau may already be attributed to the physical interaction, the contribution of the carbodiimide-mediated amidation reaction is obviously observed at the high temperature plateau for 150 EK (Fig. 4c). For the highest concentration (150 EK), the concentration of E50I60 (98 mg/ml) is appropriate to form a physical hydrogel network [13,22,23]; moreover, the corresponding ELR T_t is the lowest. This results in clearly observing the low temperature plateau (between 10 and 29 °C) attributed to the formation of physical hydrogel network, which can be clearly distinguished from the high temperature plateau (above 29 °C) attributed to the carbodiimide-mediated amidation network. In other words, increasing the temperature during the temperature sweep provides thermal energy that allows the thermally driven self-assembly of the amphiphilic E50I60 into a physically cross-linked network (low temperature plateau). When the temperature is high enough to provide the energy necessary to overcome the activation temperature needed for the amide bond formation, these chemical bonds begin to be produced to generate the chemically cross-linked network (high-temperature plateau).

Similar G′ values are found in the high temperature plateau for 100 EK and 150 EK. This could be attributed to the limited availability of amine and/or carboxylic groups for the chemical modification due to the steric hindrance of self-assembly of the E50I60 into the physical network [61]. This steric hindrance cannot make possible the effective performance of a higher number of crosslinks as compared to that of the crosslinks available at 100 mg/ml and 50 mg/ml. Indeed, a similar steric hindrance has been observed in other works, such as when the polyethylene glycol (PEG) molecules are employed as spacers, thus providing steric hindrance to the cross-linking of the alginate chains [62]. Also, steric hindrance has been observed to affect the thermoresponsive phase transition behaviors between poly [*N*-(1-meth-2-acryloyloxyethyl) pyrrolidone] (PMEP) and poly [*N*-(2-acryloyloxypropyl) pyrrolidone] (PAPP) [63]. Therefore, as a whole, Fig. 4 indicates that the hydrogel viscoelastic properties can be switched between two different ("high" and "low" logic) values of the storage modulus. Its corresponding overall crosslinking results from the contribution of both physically and chemically crosslinked networks related to the two formation mechanisms of the hydrogel. As a consequence, a tunable viscoelasticity is available using temperature as a control parameter. Furthermore, the swing of the switching is modulated by concentration.

The prepared ELRs hydrogels have the potential to be employed as injectable biomimetic dynamic hydrogels for various biomedical applications, including tissue engineering and drug delivery [64–69]. Specifically, they could be beneficial for the treatment of intervertebral disc (IVD) degeneration (caused by the dehydration of its central region called nucleus pulpous (NP)), and therefore changing the biomechanical properties of the disc [66–70]. Currently, invasive procedures such as discectomy followed by surgical vertebral fusion are the gold standard in the management of IVD degeneration [70,71]. However, these procedures can lead to further degeneration of the disc, despite providing temporary relief from lower back pain [71]. As an alternative, hydrogels have been investigated as a replacement for the NP, as they can mimic both the native composition (high water content) and the mechanical behavior (high load and shear tolerance) of the disc [66–68,70]. The main criterion for selecting the appropriate hydrogel material is to resemble the natural chemical composition, aiming for functional restoration of the IVD. Natural biomaterials such as collagen and elastin, which are present in the nucleus pulposus [72], have been integrated into treatment strategies for IVD degeneration [66–70]. The success was rendered by their undesirable mechanical properties that were partially solved through the use of cross-linkers which at the same time imposed cytotoxicity [69,73]. The most critical limitation is their rapid degradation rates as they are susceptible to catalytic enzymes present in the IVD namely collagenase and elastase. Yet, dynamic ELRs hydrogels with tunable viscoelastic properties should be exploited for the nucleus pulposus regeneration. The formation conditions and viscoelastic properties of the hydrogel matrix presented in the present study make them promising for this application. Thus, the presented hydrogel matrix is based on polymers inspired by the natural elastin protein, which provides unique mechanical properties in terms of strength and extensibility [28,74]. Additionally, a biomimetic amidation reaction using a non-toxic EDAC cross-linker has been employed to enhance the mechanical features of the hydrogels. Importantly, the hydrogels can be formed after injection, as the amidation reaction can be initiated at physiological temperature (37 °C). Overall, these hydrogels could have the potential to closely mimic the natural nucleus pulposus and rehydrate the discs of patients suffering from this disease with a minimally invasive treatment approach.

Moreover, prior to the initiation of the amidation reaction, it would be possible to mix the mesenchymal stem cells (MSCs) with the hydrogel component elements. A strategy of cell-based IVD regenerative therapy has growing evidence of success at the clinical level. For IVD regenerative purposes, bone marrow mesenchymal stem cells (MSCs) are intensively studied not just at the in vitro and in vivo levels, but also at advanced phases of clinical trials [75]. As a result, injectable hydrogels that are loaded with mesenchymal stem cells (MSCs) could be generated to restore the biomechanical characteristics of the IVD and promote tissue regeneration [68]. Co-administration of growth factors such as transforming growth factor beta (TGF-β) has enhanced MSCs differentiation and proliferation towards nucleus pulposus (NP)-like phenotype [76]. Additionally, reports have confirmed that delivering MSCs through hydrogels is associated with a significant reduction in the IVD degeneration and favored for its ability of co-delivery assuring a synergistic effect [68]. Thus, the injection of these hydrogels into specific anatomical sites, responding dynamically at physiological conditions, opens up exciting possibilities for targeted therapies.

5. Conclusions

Tunable viscoelastic ELR hydrogels have been successfully prepared in aqueous solutions using an *"in-situ"*, one-pot, fast and cost-effective process. This is attributed to the ability of carboxylic groups from glutamic acid distributed along the E50 hydrophilic block of the amphiphilic E50I60 ELR to form amide bonds with amine groups, as demonstrated with the reaction with aniline molecules in aqueous solution using the water-soluble EDAC, with a high conversion (high coupling ratio, 70%, according to the results from ^{1}H NMR and MALDI-ToF spectroscopies). Under the specific experimental conditions used, both the ELR structure and the chemical environment of the polymer chain may contribute to the high yield obtained, improving the activation of the carboxylic groups. By means of this approach, *"in-situ"* cross-linking of copolymer E50I60 with lysine-rich VKV24 ELR has resulted in the generation of viscoelastic hydrogels. The hydrogel characterization was carried out by SEM indicating a homogeneous concentration-dependent porous structure with a high level of interconnectivity. Rheological analysis shows that the evolution of the elastic G' and viscous G'' moduli is affected by the temperature and the ELR concentration. Furthermore, the gelation process is associated with a dual mechanism, as confirmed by the presence of two temperature sweep plateaus in the rheological analysis. While the low-temperature plateau is assigned to the thermally driven self-assembly of E50I60 into physical networks, the high-temperature plateau is attributed to the formation of the covalent ELR network through the formation of amide bonds. The swing of G' between the two plateaus is dependent on both the ELR hydrogel concentration and temperature. Thus, the synergistic combination between the physical network—provided by the self-assembly of the hydrophobic I60 block through the hydrophobic interactions— with the covalent network—due to the formed amide bonds between the hydrophilic E50 blocks and VKV24 ELR—is the key to generating viscoelastic hydrogels with tunable properties using concentration and temperature as control parameters. The prepared hydrogels have the potential to be employed as injectable biomimetic dynamic hydrogels for various biomedical applications, such as targeted therapies or tissue engineering including the regeneration of nucleus pulpous in the treatment of intervertebral disc degeneration.

CRediT authorship contribution statement

M. Hamed Misbah: Writing – review & editing, Writing – original draft, Methodology, Investigation, Formal analysis, Data curation, Conceptualization. **Luis Quintanilla-Sierra:** Writing – review & editing, Writing – original draft, Methodology, Investigation. **Matilde Alonso:** Writing – review & editing, Investigation, Funding acquisition. **José Carlos Rodríguez-Cabello:** Writing – review & editing, Supervision, Investigation, Funding acquisition, Conceptualization. **Mercedes Santos:** Writing – review & editing, Writing – original draft, Supervision, Investigation, Funding acquisition, Conceptualization.

Declaration of competing interest

The authors declare that they have no known competing financial interests or personal relationships that could have appeared to influence the work reported in this paper.

Data availability

No data was used for the research described in the article.

Acknowledgments

The authors are grateful for the funding from the Spanish Government (PID2019-110709RB-I00, PID2020-118669RA-I00, PID2021-122444OB-I00) and Centro en Red de Medicina Regenerativa y Terapia Celular de Castilla y León.

The author M. Hamed Misbah is funded by a full scholarship (2019–2020) from the Ministry of Higher Education of the Arab Republic of Egypt.

Appendix A. Supplementary data

Supplementary data to this article can be found online at https://doi.org/10.1016/j.mtbio.2024.100999.

References

[1] J. Lim, Q. Lin, K. Xue, X. Loh, Recent advances in supramolecular hydrogels for biomedical applications, Mater. Today Adv. 3 (2019) 100021.
[2] Y. Mao, P. Li, J. Yin, Y. Bai, H. Zhou, X. Lin, H. Yang, L. Yang, Starch-based adhesive hydrogel with gel-point viscoelastic behavior and its application in wound sealing and hemostasis, J. Mater. Sci. Technol. 63 (2021) 228–235.
[3] Z. Wu, Z. Yang, D. Sha, Y. Ma, B.Y. Kim, W. Jiang, Y. Yuan, C. Liu, Injectable, viscoelastic hydrogel precisely regulates developmental tissue regeneration, Chem. Eng. J. 434 (2022) 133860.
[4] S. Tang, B.M. Richardson, K.S. Anseth, Dynamic covalent hydrogels as biomaterials to mimic the viscoelasticity of soft tissues, Prog. Mater. Sci. 120 (2021) 100738.
[5] H. Jia, X. Lin, D. Wang, J. Wang, Q. Shang, X. He, K. Wu, B. Zhao, P. Peng, H. Wang, Injectable hydrogel with nucleus pulposus-matched viscoelastic property prevents intervertebral disc degeneration, J. Orthop. Translat. 33 (2022) 162–173.
[6] Z. Mousavikhamene, G.C. Schatz, Engineering viscoelasticity in autoregulatory nanoscale wrinkling bilayer hydrogel systems: pressure sensors and thermal-responsive drug delivery systems, ACS Appl. Nano Mater. 5 (2022) 13649–13658.
[7] O. Chaudhuri, Viscoelastic hydrogels for 3D cell culture, Biomater. Sci. 5 (2017) 1480–1490.
[8] D. Caccavo, S. Cascone, G. Lamberti, A. Barba, Hydrogels: experimental characterization and mathematical modelling of their mechanical and diffusive behaviour, Chem. Soc. Rev. 47 (2018) 2357–2373.
[9] L.J. Dooling, M.E. Buck, W.B. Zhang, D.A. Tirrell, Programming molecular association and viscoelastic behavior in protein networks, Adv. Mater. 28 (2016) 4651–4657.
[10] V.G. Muir, J.A. Burdick, Chemically modified biopolymers for the formation of biomedical hydrogels, Chem. Rev. 121 (2020) 10908–10949.
[11] S. Roberts, M. Dzuricky, A. Chilkoti, Elastin-like polypeptides as models of intrinsically disordered proteins, FEBS Lett. 589 (2015) 2477–2486.
[12] S. Acosta, L. Poocza, L. Quintanilla-Sierra, J.C. Rodríguez-Cabello, Charge density as a molecular modulator of nanostructuration in intrinsically disordered protein polymers, Biomacromolecules 22 (2020) 158–170.
[13] M.H. Misbah, L. Quintanilla, M. Alonso, J.C. Rodríguez-Cabello, Evolution of amphiphilic elastin-like co-recombinamer morphologies from micelles to a lyotropic hydrogel, Polymer 81 (2015) 37–44.

[14] J. Rodríguez-Cabello, A. Girotti, A. Ribeiro, F. Arias, Synthesis of genetically engineered protein polymers (recombinamers) as an example of advanced self-assembled smart materials, in: M. Navarro, J.A. Planell (Eds.), Nanotechnology in Regenerative Medicine, Humana Press, 2012, pp. 17–38.
[15] T. Christensen, W. Hassouneh, K. Trabbic-Carlson, A. Chilkoti, Predicting transition temperatures of elastin-like polypeptide fusion proteins, Biomacromolecules 14 (2013) 1514–1519.
[16] L. Bataille, W. Dieryck, A. Hocquellet, C. Cabanne, K. Bathany, S. Lecommandoux, B. Garbay, E. Garanger, Recombinant production and purification of short hydrophobic Elastin-like polypeptides with low transition temperatures, Protein Expr. Purif. 121 (2016) 81–87.
[17] T. Yamaoka, T. Tamura, Y. Seto, T. Tada, S. Kunugi, D.A. Tirrell, Mechanism for the phase transition of a genetically engineered elastin model peptide (VPGIG)40 in aqueous solution, Biomacromolecules 4 (2003) 1680–1685.
[18] D.W. Urry, Physical chemistry of biological free energy transduction as demonstrated by elastic protein-based polymers, J. Phys. Chem. B 101 (1997) 11007–11028.
[19] A. Girotti, J. Reguera, F.J. Arias, M. Alonso, A.M. Testera, J.C. Rodríguez-Cabello, Influence of the molecular weight on the inverse temperature transition of a model genetically engineered elastin-like pH-responsive polymer, Macromolecules 37 (2004) 3396–3400.
[20] I.G. de Torre, M. Santos, L. Quintanilla, A. Testera, M. Alonso, J.C.R. Cabello, Elastin-like recombinamer catalyst-free click gels: characterization of poroelastic and intrinsic viscoelastic properties, Acta Biomater. 10 (2014) 2495–2505.
[21] C. García-Arévalo, M. Pierna, A. Girotti, F.J. Arias, J.C. Rodríguez-Cabello, A comparative study of cell behavior on different energetic and bioactive polymeric surfaces made from elastin-like recombinamers, Soft Matter 8 (2012) 3239–3249.
[22] A. Fernández-Colino, F.J. Arias, M. Alonso, J.C. Rodríguez-Cabello, Self-organized ECM-mimetic model based on an amphiphilic multiblock silk-elastin-like corecombinamer with a concomitant dual physical gelation process, Biomacromolecules 15 (2014) 3781–3793.
[23] A. Fernández-Colino, F.J. Arias, M. Alonso, J.C. Rodríguez-Cabello, Amphiphilic elastin-like block co-recombinamers containing leucine zippers: cooperative interplay between both domains results in injectable and stable hydrogels, Biomacromolecules 16 (2015) 3389–3398.
[24] D.H. Le, A. Sugawara-Narutaki, Elastin-like polypeptides as building motifs toward designing functional nanobiomaterials, Mol. Syst. Des. Eng. 4 (2019) 545–565.
[25] J.C. Rodríguez-Cabello, I.G. de Torre, A. Ibañez-Fonseca, M. Alonso, Bioactive scaffolds based on elastin-like materials for wound healing, Adv. Drug Deliv. Rev. 129 (2018) 118–133.
[26] R.E. Sallach, W. Cui, J. Wen, A. Martinez, V.P. Conticello, E.L. Chaikof, Elastin-mimetic protein polymers capable of physical and chemical crosslinking, Biomaterials 30 (2009) 409–422.
[27] N. Annabi, S.M. Mithieux, G. Camci-Unal, M.R. Dokmeci, A.S. Weiss, A. Khademhosseini, Elastomeric recombinant protein-based biomaterials, Biochem. Eng. J. 77 (2013) 110–118.
[28] D.L. Nettles, A. Chilkoti, L.A. Setton, Applications of elastin-like polypeptides in tissue engineering, Adv. Drug Deliv. Rev. 62 (2010) 1479–1485.
[29] D.E. Berning, K.V. Katti, C.L. Barnes, W.A. Volkert, Chemical and biomedical motifs of the reactions of hydroxymethylphosphines with amines, amino acids, and model peptides, J. Am. Chem. Soc. 121 (1999) 1658–1664.
[30] D.L. Nettles, K. Kitaoka, N.A. Hanson, C.M. Flahiff, B.A. Mata, E.W. Hsu, A. Chilkoti, L.A. Setton, In situ crosslinking elastin-like polypeptide gels for application to articular cartilage repair in a goat osteochondral defect model, Tissue Eng. 14 (2008) 1133–1140.
[31] A. Heinz, C.U. Schräder, S. Baud, F.W. Keeley, S.M. Mithieux, A.S. Weiss, R. H. Neubert, C.E. Schmelzer, Molecular-level characterization of elastin-like constructs and human aortic elastin, Matrix Biol. 38 (2014) 12–21.
[32] D.W. Lim, D.L. Nettles, L.A. Setton, A. Chilkoti, Rapid cross-linking of elastin-like polypeptides with (hydroxymethyl) phosphines in aqueous solution, Biomacromolecules 8 (2007) 1463–1470.
[33] J.E. Gough, C.A. Scotchford, S. Downes, Cytotoxicity of glutaraldehyde crosslinked collagen/poly (vinyl alcohol) films is by the mechanism of apoptosis, J. Biomed. Mater. Res.: An Off. J. Soc. Biomater., The Jpn Soc. Biomater. The Aust. Soc. Biomater. Korean Soc. Biomater. 61 (2002) 121–130.
[34] M.H. Misbah, M. Santos, L. Quintanilla, C. Günter, M. Alonso, A. Taubert, J. C. Rodríguez-Cabello, Recombinant DNA technology and click chemistry: a powerful combination for generating a hybrid elastin-like-statherin hydrogel to control calcium phosphate mineralization, Beilstein J. Nanotechnol. 8 (2017) 772–783.
[35] A.M. Testera, A. Girotti, I.G. de Torre, L. Quintanilla, M. Santos, M. Alonso, J. C. Rodríguez-Cabello, Biocompatible elastin-like click gels: design, synthesis and characterization, J. Mater. Sci. Mater. Med. 26 (2015) 1–13.
[36] Z. Guo, Y. Xu, L. Dong, M.S. Desai, J. Xia, M. Liang, S.-W. Lee, S. Mi, W. Sun, Design of functional hydrogels using smart polymer based on elastin-like polypeptides, Chem. Eng. J. 435 (2022) 135155.
[37] S. Gao, Z. Yuan, W. Guo, M. Chen, S. Liu, T. Xi, Q. Guo, Comparison of glutaraldehyde and carbodiimides to crosslink tissue engineering scaffolds fabricated by decellularized porcine menisci, Mater. Sci. Eng. C 71 (2017) 891–900.
[38] K. Ulubayram, E. Aksu, S.I.D. Gurhan, K. Serbetci, N. Hasirci, Cytotoxicity evaluation of gelatin sponges prepared with different cross-linking agents, J. Biomater. Sci. Polym. Ed. 13 (2002) 1203–1219.
[39] J. Redmond, H.O. McCarthy, P. Buchanan, T.J. Levingstone, N.J. Dunne, Development and characterisation of 3D collagen-gelatin based scaffolds for breast cancer research, Biomater. Adv. (2022) 213157.
[40] L. Salvatore, M. Madaghiele, C. Parisi, F. Gatti, A. Sannino, Crosslinking of micropatterned collagen-based nerve guides to modulate the expected half-life, J. Biomed. Mater. Res. 102 (2014) 4406–4414.
[41] A.M. Testera, M. Santos, A. Girotti, F.J. Arias, J.M. Báñez, M. Alonso, J. C. Rodríguez-Cabello, A novel lipase-catalyzed method for preparing ELR-based bioconjugates, Int. J. Biol. Macromol. 121 (2019) 752–759.
[42] R. Alvarez-Rodríguez, F.J. Arias, M. Santos, A.M. Testera, J.C. Rodríguez-Cabello, Gold tailored photosensitive elastin-like polymer: synthesis of temperature, pH and UV-vis sensitive probes, Macromol. Rapid Commun. 31 (2010) 568–573.
[43] M. Alonso, V. Reboto, L. Guiscardo, A. San Martin, J. Rodríguez-Cabello, Spiropyran derivative of an elastin-like bioelastic polymer: photoresponsive molecular machine to convert sunlight into mechanical work, Macromolecules 33 (2000) 9480–9482.
[44] T.T. Tung, J. Nielsen, Amide bond formation in aqueous solution: direct coupling of metal carboxylate salts with ammonium salts at room temperature, Org. Biomol. Chem. 19 (2021) 10073–10080.
[45] C. García-Arévalo, J.F. Bermejo-Martín, L. Rico, V. Iglesias, L. Martín, J. C. Rodríguez-Cabello, F.J. Arias, Immunomodulatory nanoparticles from elastin-like recombinamers: single-molecules for tuberculosis vaccine development, Mol. Pharm. 10 (2013) 586–597.
[46] M.H. Misbah, M. Espanol, L. Quintanilla, M. Ginebra, J.C. Rodríguez-Cabello, Formation of calcium phosphate nanostructures under the influence of self-assembling hybrid elastin-like-statherin recombinamers, RSC Adv. 6 (2016) 31225–31234.
[47] D. Juanes-Gusano, M. Santos, V. Reboto, M. Alonso, J.C. Rodríguez-Cabello, Self-assembling systems comprising intrinsically disordered protein polymers like elastin-like recombinamers, J. Pept. Sci. 28 (2022) e3362.
[48] C. Gonzalez-Obeso, J. Rodriguez-Cabello, D.L. Kaplan, Fast and reversible crosslinking of a silk elastin-like polymer, Acta Biomater. 141 (2022) 14–23.
[49] S. Salinas-Fernandez, M. Santos, M. Alonso, L. Quintanilla, J.C. Rodríguez-Cabello, Genetically engineered elastin-like recombinamers with sequence-based molecular stabilization as advanced bioinks for 3D bioprinting, Appl. Mater. Today 18 (2020) 100500.
[50] I.G. de Torre, M. Weber, L. Quintanilla, M. Alonso, S. Jockenhoevel, J.C.R. Cabello, P. Mela, Hybrid elastin-like recombinamer-fibrin gels: physical characterization and in vitro evaluation for cardiovascular tissue engineering applications, Biomater. Sci. 4 (2016) 1361–1370.
[51] K.L. Spiller, S.J. Laurencin, D. Charlton, S.A. Maher, A.M. Lowman, Superporous hydrogels for cartilage repair: evaluation of the morphological and mechanical properties, Acta Biomater. 4 (2008) 17–25.
[52] A. Fernández-Colino, F. Wolf, S. Rütten, J.C. Rodríguez-Cabello, S. Jockenhoevel, P. Mela, Combining catalyst-free click chemistry with coaxial electrospinning to obtain long-term, water-stable, bioactive elastin-like fibers for tissue engineering applications, Macromol. Biosci. 18 (2018) 1800147.
[53] A. Fernández-Colino, F. Wolf, H. Keijdener, S. Rütten, T. Schmitz-Rode, S. Jockenhoevel, J.C. Rodríguez-Cabello, P. Mela, Macroporous click-elastin-like hydrogels for tissue engineering applications, Mater. Sci. Eng. C 88 (2018) 140–147.
[54] Y. Ning, S. Wang, M. Li, J. Han, C. Zhu, J. Xie, Site-specific Umpolung amidation of carboxylic acids via triplet synergistic catalysis, Nat. Commun. 12 (2021) 4637.
[55] G. Li, M. Szostak, Highly selective transition-metal-free transamidation of amides and amidation of esters at room temperature, Nat. Commun. 9 (2018) 4165.
[56] M.T. Sabatini, V. Karaluka, R.M. Lanigan, L.T. Boulton, M. Badland, T.D. Sheppard, Protecting-group-free amidation of amino acids using lewis acid catalysts, Chem.–Eur. J. 24 (2018) 7033–7043.
[57] H. Lundberg, F. Tinnis, N. Selander, H. Adolfsson, Catalytic amide formation from non-activated carboxylic acids and amines, Chem. Soc. Rev. 43 (2014) 2714–2742.
[58] E. Valeur, M. Bradley, Amide bond formation: beyond the myth of coupling reagents, Chem. Soc. Rev. 38 (2009) 606–631.
[59] T. Krause, S. Baader, B. Erb, L.J. Gooßen, Atom-economic catalytic amide synthesis from amines and carboxylic acids activated in situ with acetylenes, Nat. Commun. 7 (2016) 11732.
[60] M.T. Sabatini, L.T. Boulton, T.D. Sheppard, Borate esters: simple catalysts for the sustainable synthesis of complex amides, Sci. Adv. 3 (2017) e1701028.
[61] P. Wipf, E.M. Skoda, A. Mann, Conformational Restriction and Steric Hindrance in Medicinal Chemistry, the Practice of Medicinal Chemistry, Elsevier, 2015, pp. 279–299.
[62] O. Chaudhuri, L. Gu, D. Klumpers, M. Darnell, S.A. Bencherif, J.C. Weaver, N. Huebsch, H.-p. Lee, E. Lippens, G.N. Duda, Hydrogels with tunable stress relaxation regulate stem cell fate and activity, Nat. Mater. 15 (2016) 326–334.
[63] P. Liu, L. Xiang, Q. Tan, H. Tang, H. Zhang, Steric hindrance effect on thermoresponsive behaviors of pyrrolidone-based polymers, Polym. Chem. 4 (2013) 1068–1076.
[64] Y. Li, G. Huang, X. Zhang, L. Wang, Y. Du, T.J. Lu, F. Xu, Engineering cell alignment in vitro, Biotechnol. Adv. 32 (2014) 347–365.
[65] I. Singha, A. Basu, Chitosan based injectable hydrogels for smart drug delivery applications, Sensors Int. 3 (2022) 100168.
[66] A.E. Leckie, M.K. Akens, K.A. Woodhouse, A.J. Yee, C.M. Whyne, Evaluation of thiol-modified hyaluronan and elastin-like polypeptide composite augmentation in early-stage disc degeneration: comparing 2 minimally invasive techniques, Spine 37 (2012) E1296–E1303.

[67] R.D. Bowles, R.M. Williams, W.R. Zipfel, L.J. Bonassar, Self-assembly of aligned tissue-engineered annulus fibrosus and intervertebral disc composite via collagen gel contraction, Tissue Eng. 16 (2010) 1339–1348.
[68] Y. Gan, S. Li, P. Li, Y. Xu, L. Wang, C. Zhao, B. Ouyang, B. Tu, C. Zhang, L. Luo, A controlled release codelivery system of MSCs encapsulated in dextran/gelatin hydrogel with TGF-β3-loaded nanoparticles for nucleus pulposus regeneration, Stem Cell. Int. (2016) 2016.
[69] A. Pandit, D. O'Halloran, L. Calderon, E. Collin, M. Murphy, Type II Collagen-Hyaluronan Hydrogel-A Step towards a Scaffold for Intervertebral Disc Tissue Engineering, 2010.
[70] C.C. Guterl, E.Y. See, S.B. Blanquer, A. Pandit, S.J. Ferguson, L.M. Benneker, D. W. Grijpma, D. Sakai, D. Eglin, M. Alini, Challenges and strategies in the repair of ruptured annulus fibrosus, Eur. Cell. Mater. 25 (2013) 1.
[71] B.s. Xu, Y. Liu, H.w. Xu, Q. Yang, X.l. Ma, Y.c. Hu, Intervertebral fusion with Mobile Microendoscopic discectomy for lumbar degenerative disc disease, Orthop. Surg. 8 (2016) 241–245.
[72] J. Yu, U. Tirlapur, J. Fairbank, P. Handford, S. Roberts, C.P. Winlove, Z. Cui, J. Urban, Microfibrils, elastin fibres and collagen fibres in the human intervertebral disc and bovine tail disc, J. Anat. 210 (2007) 460–471.
[73] S.S. Sivan, A.J. Hayes, E. Wachtel, B. Caterson, Y. Merkher, A. Maroudas, S. Brown, S. Roberts, Biochemical composition and turnover of the extracellular matrix of the normal and degenerate intervertebral disc, Eur. Spine J. 23 (2014) 344–353.
[74] R. Petitdemange, E. Garanger, L. Bataille, K. Bathany, B. Garbay, T.J. Deming, S. Lecommandoux, Tuning thermoresponsive properties of cationic elastin-like polypeptides by varying counterions and side-chains, Bioconjugate Chem. 28 (2017) 1403–1412.
[75] G. Vadalà, F. Russo, L. Ambrosio, M. Loppini, V. Denaro, Stem cells sources for intervertebral disc regeneration, World J. Stem Cell. 8 (2016) 185.
[76] X. Zhou, Y. Tao, J. Wang, C. Liang, J. Wang, H. Li, Q. Chen, Roles of FGF-2 and TGF-beta/FGF-2 on differentiation of human mesenchymal stem cells towards nucleus pulposus-like phenotype, Growth Factors 33 (2015) 23–30.